

# Electrochemical promotion of ethanol partial oxidation and reforming reactions for hydrogen production

Arash Fellah Jahromi <sup>a,1</sup>, Estela Ruiz-López <sup>b,1</sup>, Fernando Dorado <sup>b</sup>, Elena A. Baranova <sup>a</sup>, Antonio de Lucas-Consuegra <sup>b\*</sup>

<sup>a</sup>Department of Chemical and Biological Engineering, Centre for Catalysis Research and Innovation (CCRI), University of Ottawa, 161 Louis-Pasteur, Ottawa, ON, K1N 6N5, Canada

<sup>b</sup>Department of Chemical Engineering, School of Chemical Sciences and Technologies, University of Castilla-La Mancha, Avenida Camilo José Cela 12, 13005 Ciudad Real, Spain

<sup>1</sup>These authors contributed equally to this work.

\* Corresponding author's email: [Antonio.LConsuegra@uclm.es](mailto:Antonio.LConsuegra@uclm.es)

## Abstract

The electrochemical activation of a Pt-K $\beta$ Al<sub>2</sub>O<sub>3</sub> catalytic system is studied for hydrogen production from ethanol. The in-situ intercalation of potassium ions onto the catalyst surface under negative polarization leads to hydrogen activation and an increase in the production rate under all explored conditions, observing a reproducible, controllable and reversible effect. Under ethanol partial oxidation conditions, the ions migration promotes oxidation dehydrogenation route vs. ethanol dehydration one. Moreover, the steam addition is evaluated through different reaction conditions: steam reforming, partial oxidation and autothermal reforming. The steam reforming reaction exhibits the highest initial catalytic activity; although a strong deactivation of the catalyst occurs due to carbonaceous species deposition. Comparing partial oxidation and autothermal reforming, the latter one presents the highest catalytic activity and the strongest electrochemical activation effect. These findings contribute to the Electrochemical Promotion of Catalysis phenomenon application to operando tuning the catalyst conversion towards hydrogen production, therefore expanding its application to hydrogen technology.

**Keywords:** *electrochemical promotion, ethanol partial oxidation, hydrogen production, ethanol autothermal reforming, ethanol steam reforming*

## 1 **1. Introduction**

2 Hydrogen nexus is a corner stone for a sustainable energy future to address both ever-growing  
3 energy demand and minimizing greenhouse gas (GHG) emission [1]. Hydrogen is as an excellent  
4 alternative to conventional fuels, because it has the highest specific energy among fossil fuels [2],  
5 and its production from biomass derived feedstocks like alcohols could contribute to lowering  
6 GHG emission [3].

7 Bio-ethanol has an industrial potential as the feedstock for hydrogen generation via low carbon  
8 processes, thanks to its easy storage, lower volatility, high hydrogen content per mole, absence of  
9 toxicity, abundance of biomass feedstocks as well as safe transport and handling [4,5]. Various  
10 processes exist for ethanol conversion to hydrogen such as aqueous phase reforming, dry  
11 reforming, steam reforming (SR), partial oxidation (POX), and autothermal reforming (ATR) [3,6–  
12 8], being the last three the most tenable options [3]. SR reaction offers higher energy efficiency  
13 since provides the maximum theoretical yield of hydrogen [9] although is a strongly endothermic  
14 process that requires an external supply of heat. POX reaction shows a fast start-up and quick  
15 response time, as well as a simple and compact design, which is desirable for automotive and  
16 mobile fuel cell applications [10]. However, the likelihood of hot-spot formation makes it difficult  
17 to control the reaction. Although being exothermic is an innate property of POX reactions, its  
18 major barriers can be expressed as relatively low hydrogen mole produced per mole of ethanol [3].  
19 Oxidative steam reforming or autothermal reforming process is the combination of steam  
20 reforming and partial oxidation reactions. The addition of oxygen to steam reforming conditions  
21 allows achieving an equilibrium between hydrogen selectivity and energy efficiency, besides  
22 promoting the removal of inactive carbon species from the catalyst surface [11]. Therefore,  
23 proposing a solution to prevail the challenges of SR, POX, and ATR of ethanol comes into  
24 consideration. Such a solution requires to meet both objectives of increasing catalytic rate of  
25 favorable product (hydrogen) and minimizing coke formation.

26 Diverse catalytic systems have been investigated for catalytic steam reforming, including  
27 transition metals (Co, Cu, Ni) [12–14], noble metals (Pd, Au, Ru, Pt, Rh) [12,15], and bimetallic  
28 and ternary metallic combination of transition and noble metals [16,17]. Similar, several catalytic  
29 systems, such as packed or fluidized bed reactors or fluidized bed membrane reactors [18,19], with  
30 the focus on noble metals or transition metals were proposed for ATR [20–22]. However, both SR

1 and ATR of ethanol suffer from several limitations and challenges such as: i) catalyst deactivation  
2 [23], ii) formation of undesirable by-products (e.g. CH<sub>4</sub>) [24], and iii) continuous heat supply  
3 especially for SR reactions [3].

4 On the other hand, and although POX reaction has not been so widely studied in different catalytic  
5 systems, the role of noble metals (Pt, Rh, Pd, Ru) [10,25] as well as non-noble metals (Ni, Co)  
6 [10,26] has been explored for their use as monometallic and bimetallic catalysts [27,28]. Moreover,  
7 the application of catalytic promoters could further enhance ethanol conversion to hydrogen. In  
8 the case of POX reaction, it was found that the addition of a V<sub>2</sub>O<sub>5</sub> phase to a Pt catalyst improved  
9 its performance due to the V<sub>2</sub>O<sub>5</sub> redox properties [29]. It was demonstrated that nitrogen promoted  
10 the catalytic activity of partial oxidation processes over vanadium oxide catalyst supported on  
11 nitrogen-doped TiO<sub>2</sub> [30]. Chimentao et al. [31] also explored the function of alkali promoter, Na,  
12 in a vanadium oxide catalyst. Sodium addition affected dispersion, reducibility and acidity of the  
13 catalyst and, although a high amount of sodium worked against catalytic activity, an increase in  
14 sodium loading decreased carbon deposition during reaction, extending catalyst lifetime.

15 The phenomenon of electrochemical promotion of catalysis (EPOC), also referred as non-faradic  
16 electrochemical modification of catalytic activity (NEMCA) [32,33], is described as an activation  
17 of a catalyst via back-spillover mechanism in which the promoter ions are supplied from an electro-  
18 active support (solid electrolyte) by introduction of a potential difference between support and  
19 surface of catalyst or electro polarization. Accordingly, the in-situ supply/removal of promoters  
20 can be continuously and reversibly controlled, under reaction condition. According to the recent  
21 literature, EPOC can contribute in solving various challenges faced in heterogeneous catalysis  
22 domain such as to alter the oxidation state of a catalyst, reversibly [34–36], to utilize carbon  
23 deposition for regeneration of a catalyst throughout the catalytic reaction [37], and to hinder the  
24 poisoning effect [38].

25 Application of EPOC resulted in electrochemical activation of various catalytic systems with the  
26 purpose of the hydrogen production. The processes of concern were methanol steam reforming  
27 [38,39], water-gas shift (WGS) [40,41], and methane steam reforming [42,43] reactions. SR of  
28 methanol can be the most relevant case to ethanol reforming as both feedstocks categorized as  
29 primary alcohols, and the studied catalytic systems were Ni and Cu both supported on K $\beta$ Al<sub>2</sub>O<sub>3</sub>  
30 [38,39]. Most of these studies have shown the interest of EPOC in the H<sub>2</sub> production technology

1 as reviewed in recent publications [44,45]. Nonetheless, the commercial implantation of the EPOC  
2 phenomenon has not been developed yet, being the poorly dispersed materials on the electrode,  
3 the reactor configuration or the study of the adequate processes the main drawbacks [45].

4 A recent study has also recently shown the potential application of EPOC for SR of ethanol over  
5 Pt-K $\beta$ Al<sub>2</sub>O<sub>3</sub> electrochemical catalyst. The reported increase in activity and selectivity of a Pt  
6 catalyst in H<sub>2</sub> production was due to the electrochemical supply of the potassium ions from K-  
7  $\beta$ Al<sub>2</sub>O<sub>3</sub>. This resulted in significant increase in H<sub>2</sub> production rate, and removal of intermediate  
8 carbonaceous species from the surface of catalyst via application of +2 V [46]. In addition, the  
9 complete oxidation of ethanol reaction was studied using EPOC as a tool to enhance the  
10 dehydrogenation of ethanol and the subsequent formation of acetaldehyde over Pt [47]. Tsiakaras  
11 et al.[48] also conducted a study on a similar catalytic system and optimized the reaction conditions  
12 for the maximum production of acetaldehyde. To date, no research on EPOC of the partial  
13 oxidation of ethanol has been reported.

14 The present study aims to investigate for the first time in literature the application of EPOC  
15 phenomenon to the partial oxidation of ethanol. In addition, steam reforming of ethanol was carried  
16 out to compare to what extent the results of POX and SR of ethanol are varied with respect to  
17 activity in hydrogen production. The optimal oxygen-to-ethanol and steam-to-ethanol, three  
18 atmospheres of POX, SR, and ATR were investigated to assess the influence of the EPOC  
19 phenomenon on the catalytic activity and catalytic stability. Furthermore, the reproducibility of  
20 the EPOC phenomenon was investigated under ATR conditions under five short polarization  
21 cycles and under a long-time polarization experiment to check the stability of the system in view  
22 of possible practical application.

## 23 **2. Experimental section**

### 24 **2.1. Electrochemical catalyst preparation**

25 The electrochemical catalyst used consisted of a continuous, thin Pt film supported on an alkaline  
26 solid electrolyte (K- $\beta$ Al<sub>2</sub>O<sub>3</sub>, K<sup>+</sup> conductor), as the one used in a previous study [46]. Au, which  
27 was chosen as a counter and pseudo-reference electrode due to its inertness, was first deposited on  
28 one side of a 20-mm-diameter, 1-mm-thick K- $\beta$ Al<sub>2</sub>O<sub>3</sub> (Ionotec) disc by applying a thin coat of  
29 gold paste (Gwen Electronic Materials) following by calcination at 800 °C for 2 h (heating ramp

1 of 5 °C·min<sup>-1</sup>). The working Pt electrode was deposited on the opposite side of the solid-electrolyte.  
2 Pt thin film was deposited by impregnation of a H<sub>2</sub>PtCl<sub>6</sub> water/2-propanol solution, as described  
3 in detail elsewhere [49]. Finally, the electrode was again calcinated at 550 °C for 2 h (heating ramp  
4 of 5 °C·min<sup>-1</sup>). The impregnated geometric area of the electrode was 2.01 cm<sup>2</sup> and its final Pt  
5 loading was 1 mg·cm<sup>-2</sup>. Prior to any catalytic activity measurement, a temperature programmed  
6 reduction treatment was performed. Electrocatalyst was exposed to a 5% H<sub>2</sub> stream (Ar balance,  
7 total flow = 100 mL·min<sup>-1</sup> Standard Ambient Temperature and Pressure, SATP) from room  
8 temperature to 550 °C (heating ramp of 5 °C·min<sup>-1</sup>).

9

## 10 **2.2. Catalytic activity measurements**

11 All catalytic activity measurements were carried out in an experimental setup used in previous  
12 studies [49] with a well-known single chamber solid-electrolyte cell reactor configuration [50].  
13 Two thermostated saturators, which contained ethanol (Panreac, 99.8% purity) and milli-Q water  
14 respectively, were sparged with an Ar gas flow to feed the reactor. The Ar flow was controlled by  
15 a set of mass flowmeters (Bronkhorst EL-FLOW) that in turn controlled the rest of the gases used.  
16 These reaction gases (Praxair, Inc) were certificated standards (99.999% purity) of Ar (carrier gas),  
17 H<sub>2</sub> (reducing agent), and O<sub>2</sub> (reactant gas). A double channel gas chromatograph (GC) (Bruker  
18 450-GC) previously described [46] and connected on-line was used to analyse all reactant and  
19 product gases. The detected products were hydrogen, carbon monoxide, carbon dioxide, methane,  
20 ethylene and acetaldehyde.

21 Working, counter and reference electrodes were connected to an Autolab PGSTAT320-N  
22 potentiostat-galvanostat (Metrohm Autolab) using gold wires (Alfa Aesar, 99.95% purity). In  
23 order to perform the EPOC experiments, different electric potentials were applied between  
24 working and counter electrodes and measured between working and reference electrodes ( $V_{WR}$ ),  
25 as it is generally proceeded in conventional three-electrode electrochemical cells [51,52].

26 All catalytic experiments were carried out at ambient pressure and at 550 °C, with an overall flow  
27 rate of 100 mL·min<sup>-1</sup> (SATP). Partial oxidation, steam reforming and autothermal reforming of  
28 ethanol reactions were studied by applying potentiostatic transients between +2 V and -1 V. In the  
29 case of partial oxidation reactions, different inlet compositions (O<sub>2</sub>:EtOH = 1:2, 1:3, 1:4) were

1 evaluated, keeping always a 3% ethanol composition. Ethanol steam reforming composition  
2 consisted of 3% EtOH and 9% H<sub>2</sub>O, Ar balance, whereas an inlet composition of 3% EtOH, 9%  
3 H<sub>2</sub>O, 1% O<sub>2</sub>, Ar balance was used in autothermal reforming reactions.

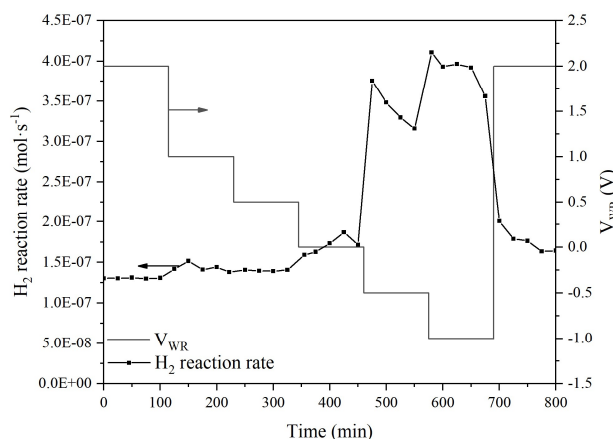
4

### 5 **3. Results and discussion**

6

#### 7 **3.1. Electrochemical promotion of Pt catalyst for the partial oxidation of ethanol**

8 The phenomenon of Electrochemical Promotion was first applied to the ethanol partial oxidation  
9 reaction. For that purpose, potentiostatic transients experiments from +2 V to -1 V (for 115 min  
10 each) were performed at 550 °C. **Figure 1** shows the response of hydrogen production rate vs. time  
11 during the application of various electrochemical potentials.



12

13 **Figure 1.** Potentiostatic transient response of hydrogen reaction rate as a function of applied potential  
14 Inlet composition: 3% EtOH, 1% O<sub>2</sub>, Ar balance. T = 550 °C.

15 At the beginning and at the end of each experiment, a positive potential ( $V_{WR} = +2$  V) was applied  
16 to clean the catalyst surface and remove any present K<sup>+</sup> ions. This initial positive potential  
17 application is required because some positive alkaline ions could spontaneously migrate to the  
18 catalyst surface during the catalyst preparation and reduction steps. This was previously reported  
19 for catalytic systems supported on alkaline ionic conductors, e.g., K- $\beta$ Al<sub>2</sub>O<sub>3</sub> [53]. After positive  
20 polarization, the catalyst film is free of potassium ions, establishing in that way an unpromoted,  
21 reference state.

1 **Figure 1** shows that a decrease in the applied potential below 0.5 V led to an increase in the  
2 hydrogen production rate, i.e., the electrochemical supply of  $K^+$  ions led to a strong activation of  
3 the partial oxidation of ethanol on the Pt catalyst. This enhancement of the hydrogen production  
4 rate through the presence of  $K^+$  ions corresponded, according to the rules of electrochemical  
5 promotion of catalysis, to an electrophilic behavior [33]. The electrophilic behavior is translated  
6 into a hydrogen production rate increase due to a decrease in catalyst potential and catalyst work  
7 function. In this case, the migration of positively charged potassium species weakened the Pt  
8 chemical bond with electron-donor adsorbates (ethanol) and strengthened chemical bond with  
9 electron-acceptor ones (oxygen). Similar behavior was reported in a previous study of methanol  
10 partial oxidation using the same solid electrolyte, where methanol was identified as the donor  
11 molecule and oxygen as the acceptor one [54].

12 On the other hand, it can be observed a relevant catalyst deactivation during the negative  
13 polarization steps. Hence, after the initial catalyst activation, there was a decrease in the activity  
14 probably due to the large formation of adsorbed intermediate reaction species. These intermediate  
15 species that would further react and be decomposed are also capable of partially blocking some  
16 the active sites. Catalyst deactivation has always been a major issue in partial oxidation reactions  
17 and a certain amount of carbon deposit was measured on different catalysts surfaces [26,27].  
18 Nonetheless, the decrease observed in **Figure 1** seems to be more likely due to an excess of acetate  
19 or ethoxy species adsorbed on the catalyst surface [11,25], which would be further reacted into  
20 acetaldehyde. In fact, an initial deactivation was observed at the beginning of the reaction in  
21 previous catalytic studies [55–57], even if the catalysts performance remained stable after this  
22 deactivation.

23 Finally, the application of +2 V at the end of the experiment resulted in removal of  $K^+$  ions from  
24 the catalyst surface back to the solid electrolyte, leading to a decrease in hydrogen production rate.  
25 The reaction rate value returned to its initial state observed at the beginning of the experiments,  
26 confirming a reversible EPOC effect. This effect was previously observed in an in-situ XPS study  
27 on a Ni catalyst supported on  $K\text{-}\beta\text{Al}_2\text{O}_3$  [58]. An intense  $K_{2p}$  signal was found under negative  
28 potential of -2 V that disappeared almost immediately when potential was switched to a positive  
29 value of +2 V. Similar hydrogen production rate values at the beginning and at the end of the

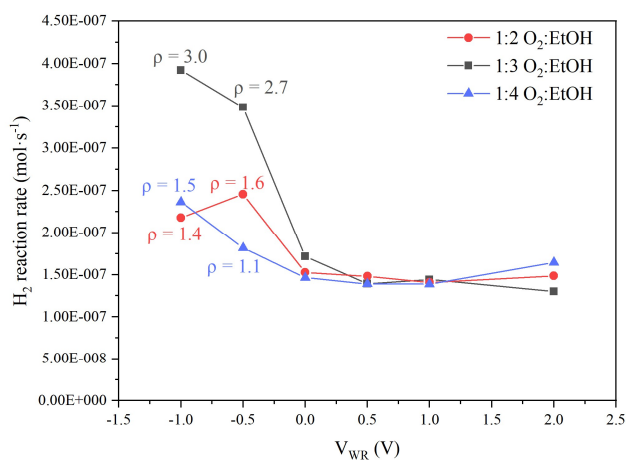
1 experiment not only showed the reversible nature of the promotional effect, but also a good  
2 stability of the catalyst film through different polarization steps.

3 Following the procedure carried out in **Figure 1**, the ratio of oxygen-to-ethanol (O<sub>2</sub>:EtOH) was  
4 studied at different applied potentials (for 115 min each) at 550 °C, as shown in **Figure 2**. Three  
5 different O<sub>2</sub>:EtOH ratios were evaluated, maintaining the composition of ethanol at 3%. In this  
6 kind of transients, a steady-state catalytic rate value was obtained after few minutes of polarization.  
7 In the cases that catalytic rate values were not stable, an average value was selected. In order to  
8 evaluate the catalyst activation under EPOC, the reaction rate enhancement ratio,  $\rho$ , was calculated  
9 using Eq. (1) [33]:

$$10 \quad \rho = \frac{r}{r_0} \quad (1)$$

11 where  $r$  denotes the promoted ( $V_{WR} < 2$ ) steady state catalytic rate value at each potential step, and  
12  $r_0$  the unpromoted ( $V_{WR} = 2$ ) catalytic rate. Under all the explored O<sub>2</sub>:EtOH molar ratios, hydrogen  
13 reaction rates values always showed an electrophilic EPOC behavior, asserting the positive  
14 influence of the potassium ions and the catalyst work function decrease. Nonetheless, in the case  
15 of 1:2 ratio, a maximum value was reached at -0.5 V. Further potential decrease to -1 V led to a  
16 decrease in the catalytic activity. At this molar ratio, a high O<sub>2</sub> coverage could be restricting ethanol  
17 adsorption on the catalyst surface. At negative potentials (-1 V), the presence of K<sup>+</sup> strengthened  
18 the Pt chemical bond with oxygen while weakening with ethanol. For that reason, ethanol  
19 molecules could be limited in the catalyst surface due to the large coverage of oxygen. On the  
20 other hand, and as previously reported while working with alkali conductors [54], Pt impregnated  
21 films could form and store potassium surface compounds, blocking part of the catalyst surface and  
22 decreasing the number of Pt active sites. In these cases, the nature of the EPOC phenomenon relies  
23 also on the electrocatalytic activity of the catalyst film and not only on the kinetics order of  
24 acceptor and donor molecules. Working at a negative potential such as -1 V could lead to an excess  
25 of promoter coverage on the catalyst surface that could poison Pt active sites [39].





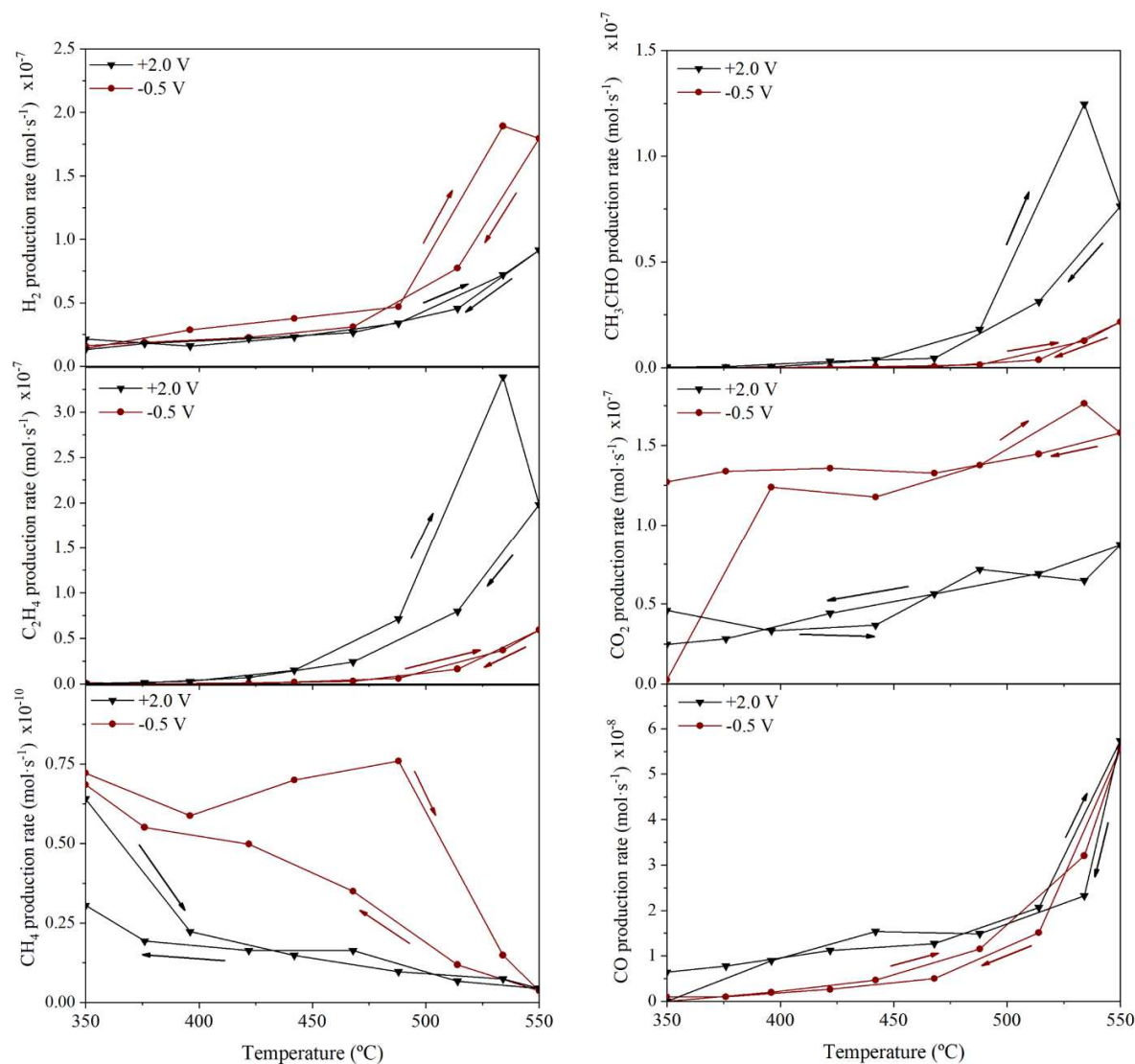
1  
 2 **Figure 2.** Hydrogen production rate and vs. applied potential at three different O<sub>2</sub>: EtOH molar ratios.  
 3 Inlet composition: 3% EtOH. T = 550 °C.

4 According to catalytic partial oxidation of ethanol studies [59], the oxygen-to ethanol molar ratio  
 5 affects directly on the hydrogen yield, which is dramatically reduced at high ratios since the  
 6 competitive hydrogen oxidation reaction is enhanced along with the ethanol complete oxidation  
 7 reaction. For that reason, O<sub>2</sub>:EtOH molar ratios below 0.5 were selected in this work, finding the  
 8 best electrocatalytic performance while feeding the reactor with 1:3 O<sub>2</sub>:EtOH molar ratio. The  
 9 migration of potassium ions favors the oxygen adsorption (electron-acceptor) rather than ethanol  
 10 adsorption (electron-donor) into the catalyst surface. Thus, high molar ratios could result in a large  
 11 coverage of oxygen that could limit the presence of ethanol in the catalyst surface while very low  
 12 molar ratios could not provide enough oxygen. For that reason, 1:3 O<sub>2</sub>:EtOH molar ratio presented  
 13 the highest catalytic activity and EPOC increase and it was selected as the optimal reaction  
 14 atmosphere for the rest of experiments. In the same way, an optimal polarization value of -0.5 V  
 15 was selected for subsequent reaction experiments since a further negative potential application of  
 16 -1 V may conditioned the long operation life of the electrochemical cell with no relevant increase  
 17 in the catalytic reaction rate.

### 18 **3.2. Insight of the promotional effect on the partial oxidation reaction mechanism**

19 The variation of the different products rates: hydrogen, carbon monoxide, carbon dioxide,  
 20 methane, ethylene and acetaldehyde at unpromoted (+2 V) and promoted (-0.5 V) conditions was  
 21 investigated through temperature programmed experiments, as shown in **Figure 3**. In these  
 22 experiments, products reaction rates were followed-up via gas chromatography while applying a

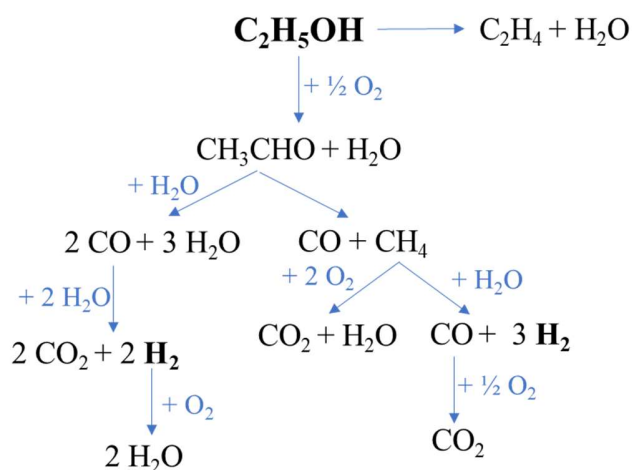
- 1 constant potential (+2 V or -0.5 V) and programming a  $2\text{ }^\circ\text{C}\cdot\text{min}^{-1}$  ramp temperature from 350  $^\circ\text{C}$
- 2 to 550  $^\circ\text{C}$  and then back to 350  $^\circ\text{C}$ .



3  
 4 **Figure 3.** Temperature programmed reaction experiments (rate =  $2\text{ }^\circ\text{C}\cdot\text{min}^{-1}$ ): Product reaction rate (as  
 5 indicated in the figure) vs. temperature at unpromoted (+2 V) and promoted (-0.5 V) conditions. Inlet  
 6 composition: 3% EtOH, 1% O<sub>2</sub>, Ar balance. T = 550  $^\circ\text{C}$ .

7  
 8 Due to the presence of a C-C bond in the ethanol molecule and the oxygen, the possible reaction  
 9 pathways that may occurred on the system are complex. In fact, Sawatmongkhon et al. [59]  
 10 proposed 21 reactions that might take place during partial oxidation of ethanol. According to  
 10

1 literature, the possible combinations due to the number of potential by-products and its further  
 2 transformations are quite numerous, and depend strongly on the support material, metal catalyst,  
 3 and on the reaction conditions [60], playing a dominant role in the scission of the C–C bond and  
 4 the final product distribution [61]. On the basis of previous studies [60,62,63] and the products  
 5 experimentally measured here, the possible reaction mechanism (schemed in **Figure 4**) could be  
 6 developed as follows. The oxidation dehydrogenation and dehydration of ethanol are the two initial  
 7 competitive steps on the reaction mechanism. Following the first route, ethanol is adsorbed on Pt  
 8 catalyst surface, where acetaldehyde is produced due to the presence of oxygen. Acetaldehyde is  
 9 then reformed and decomposed into methane and monoxide carbon, which would be further  
 10 oxidized and reformed into hydrogen.



11  
 12 **Figure 4.** Reaction mechanism scheme for partial oxidation of ethanol.

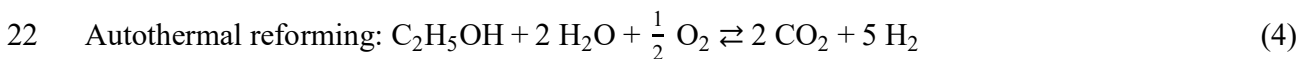
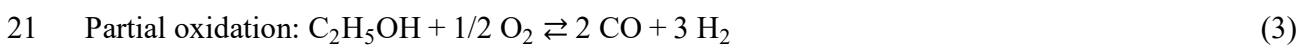
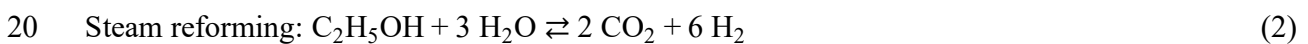
13  
 14 As observed in previous catalytic studies [56,64,65], at the explored temperature range, the  
 15 oxidation dehydrogenation and dehydration reactions can lead to noticeable amounts of  
 16 acetaldehyde, water or ethylene. In addition, the formation of carbon monoxide, which is  
 17 associated with hydrogen generation, is favored while increasing temperatures [59,64]. However,  
 18 it can be observed that the effect of the electrochemical promotion could allow its activation to  
 19 occur at lower temperatures increasing H<sub>2</sub> production. Hence, as shown in **Figure 3**, and under  
 20 unpromoted conditions (+2 V), it can be observed the pronounced increase in acetaldehyde and  
 21 ethylene production rates by temperature. The oxidation dehydrogenation and dehydration  
 22 reactions, which are the first steps of the reaction mechanism, are activated by temperature.

1 Nonetheless, this activation is not clearly observed in further reaction products such as hydrogen.  
2 Acetaldehyde reforming and decomposition reactions become the rate-limiting step, so the  
3 reaction mechanism is limited. However, the presence of  $K^+$  ions on the catalyst surface (under  
4 promoted conditions, i.e., -0.5 V) led to a strong activation of the hydrogen production rate at  
5 lower temperatures. According to these results, one could suggest that polarization activated  
6 ethanol oxidation dehydrogenation route leading to an increase in the  $H_2$  production rate instead  
7 of ethylene formation. Hence, the presence of potassium ions enhances the initial acetaldehyde  
8 formation and further reforming and decomposition reactions, and hence the rest of the  
9 mechanism, giving as a result the increase in hydrogen production rate. Since ethanol dehydration  
10 reaction route does not produce hydrogen, it was demonstrated the beneficial effect of EPOC  
11 application on partial ethanol oxidation, that favors ethanol oxidation dehydrogenation route that  
12 leads to hydrogen production instead of ethanol dehydration one.

### 13 **3.3.Effect of the steam addition: evaluation of steam reforming, partial oxidation and** 14 **autothermal reforming reaction conditions.**

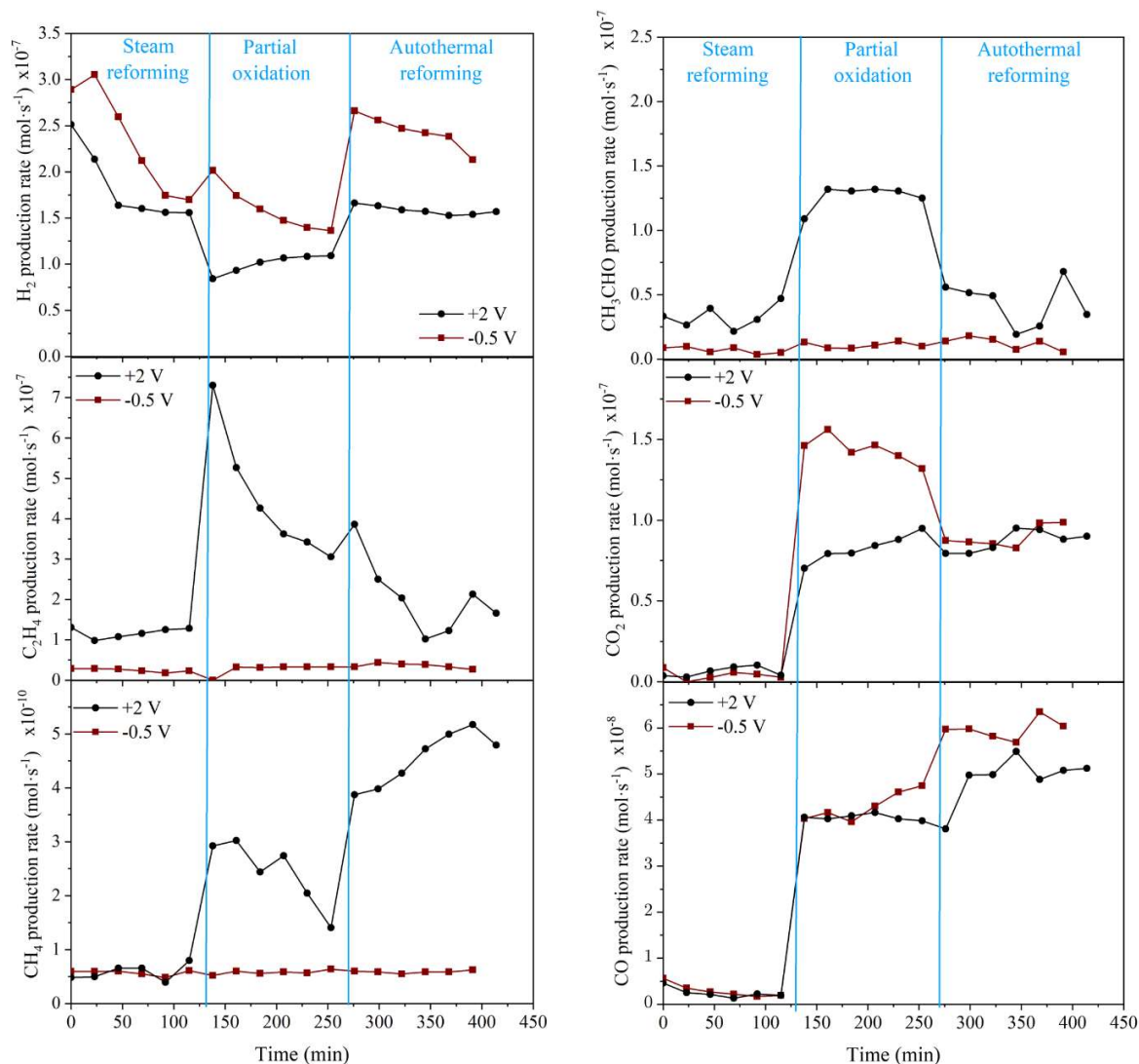
15 The effect of the addition of steam to the system was evaluated. For that purpose, three different  
16 reaction conditions: steam reforming, partial oxidation and autothermal reforming (Eq. (2-4)) were  
17 studied.

18 The production rates vs. time were followed-up under unpromoted (+2 V) and promoted conditions  
19 (-0.5 V), modifying the reaction conditions every 140 min, as shown in **Figure 5**.



23 For all three reaction conditions, the promotional effect presented an electrophilic behavior since  
24 the presence of  $K^+$  ions activated all reaction mechanism towards hydrogen production, favoring  
25 the complete conversion of intermediate products such as acetaldehyde, ethylene or methane that  
26 were not observed under promoted conditions.

27



1  
 2 **Figure 5.** Products reaction rates vs. time. Changes in the atmosphere. Steam reforming: 3% EtOH, 9%  
 3 H<sub>2</sub>O, Ar balance. Partial oxidation: 3% EtOH, 1% O<sub>2</sub>, Ar balance. Autothermal reforming: 3% EtOH, 9%  
 4 H<sub>2</sub>O, 1% O<sub>2</sub>, Ar balance. T = 550 °C.

5  
 6 As expected, under unpromoted and promoted conditions, steam reforming presented a higher  
 7 catalytic activity towards hydrogen production, since it provides the maximum theoretical yield of  
 8 hydrogen [9]. However, hydrogen production rate decreased in a more pronounced way under this  
 9 atmosphere. In a previous study, where ethanol steam reforming reaction was studied using the  
 10 same electrocatalyst configuration [46], it was observed a catalytic activity decrease along the

1 time, especially pronounced under promoted conditions. This decrease was attributed to the  
2 continuous formation and adsorption of intermediate carbonaceous species that block Pt active  
3 sites. Intermediate carbonaceous species are induced by the presence of potassium ions on the  
4 catalyst surface, being the reason of the fast decrease under promoted species.

5 Under partial oxidation conditions, and as already discussed, ethanol oxidation dehydrogenation  
6 and ethanol dehydration reactions are activated at this temperature ( $T = 550\text{ }^{\circ}\text{C}$ ), leading to large  
7 acetaldehyde and ethylene production rates under unpromoted conditions, while hydrogen  
8 production rates are limited since acetaldehyde reforming and decomposition reactions act as the  
9 rate-limiting step. Under promoted conditions, hydrogen production rates increased since the  
10 presence of  $\text{K}^+$  ions activated the acetaldehyde reforming route as previously discussed. As already  
11 observed in previous studies [26], and under unpromoted conditions, higher acetaldehyde  
12 production rates were achieved by replacing steam with oxygen, although its further  
13 decomposition was hindered leading to a decrease in hydrogen selectivity. Nonetheless, even if  
14 acetaldehyde decomposition was enhanced via polarization, partial oxidation provides a lower  
15 theoretical yield of hydrogen. Although partial oxidation showed a more stable behavior, the  
16 obtained catalytic activity is lower than the two other reactions.

17 Similar justification can be presented for CO formation rate in partial oxidation and autothermal  
18 reforming with negative potential. Compared to CO production rate, a noticeable increase can be  
19 observed under partial oxidation and autothermal reforming, though the maximum CO formation  
20 rate is approximately 2.6 and 3.6 times lower than the correlated point for hydrogen production  
21 rate under negative potential for POX and ATR. Acetaldehyde, ethylene, and methane production  
22 rate exhibited a quasi-steady state behavior in all three reaction conditions with relatively low  
23 magnitude under promoted condition. Such a behavior can prove that the catalytic activity at  
24 promoted state is independent from the exposed reaction conditions, and a small fraction of the  
25 product distribution can be associated with the abovementioned species.

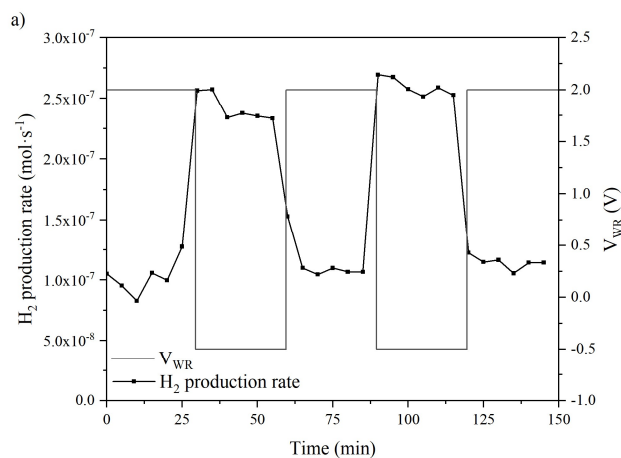
26 The combination of steam reforming and partial oxidation resulted in autothermal reforming with  
27 a pronounced increase in hydrogen formation rate; moreover, the experimentally observed  
28 catalytic deactivation is less important vs. the steam reforming conditions, due to the presence of  
29 some  $\text{O}_2$  in the gas atmospheres which favors the oxidation of intermediate and carbonaceous  
30 reactions species. Analysis of the rate enhancement ratio ( $\rho$ ) for  $\text{H}_2$  production reveals that the

1 highest value is attained under autothermal reforming conditions achieving a value of 1.6 under  
2 steady state conditions (autothermal reforming,  $\rho = 1.6$ ; steam reforming,  $\rho = 1.1$ ; partial oxidation,  
3  $\rho = 1.3$ ). Taking into account these results, the autothermal reforming conditions were selected as  
4 the optimal ones (activity, stability and magnitude of EPOC enhancement) for subsequent stability  
5 and reproducible reaction experiments, as shown below.

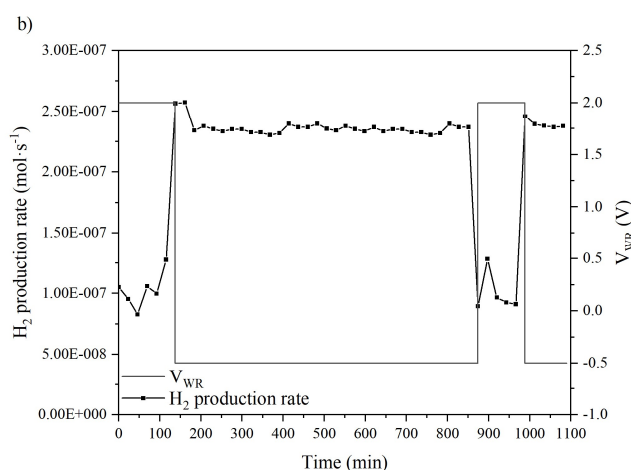
6

### 7 **3.4. Reproducibility and stability tests for autothermal reforming conditions**

8 The stability and reproducibility tests were conducted by two different kind of reaction  
9 experiments: short- and long-time polarization experiments. During short-time polarization, H<sub>2</sub>  
10 production rate was monitored through 30 min cycles in a sequence of unpromoted (+2 V)  
11 followed by promoted (- 0.5 V) state for an overall exposure time of 150 min (**Figure 6a**). Long-  
12 time polarization lasts for 1100 min with initial unpromoted step (+2V) for 150 min, subsequent  
13 promoted state (- 0.5 V) for 720 minutes (12 h), following the second unpromoted state step for  
14 120 min, and finally with the last promoted step for 110 min (**Figure 6b**).



1



2

3 **Figure 6.** Autothermal reforming stability tests: hydrogen reaction rate vs. time. a) Short-time (30 min  
 4 each) polarization cycles. b) Long-time negative polarization. Inlet composition: 3% EtOH, 9% H<sub>2</sub>O, 1%  
 5 O<sub>2</sub>, Ar balance. T = 550 °C.

6 The results of short-time polarization reveal that the attained EPOC effect is electrophilic,  
 7 reversible, and reproducible which agrees well with the findings of **Figure 5**. As it has been  
 8 remarked in all previous experiments and all different reaction conditions, the electrochemical  
 9 supply of potassium enhanced hydrogen production rate. Hence, as already observed, potassium  
 10 ions migration during the first seconds of polarization induced hydrogen production rate activation  
 11 response while switching from unpromoted to promoted states. Moreover, hydrogen production  
 12 rates were reproducible, leading to the same values while the same polarizations were applied. On  
 13 the other hand, long term negative polarization also showed similar behavior as the short-time one  
 14 with respect to EPOC effect. Contrary to the steam reforming conditions, the system shows a quasi



1 steady state H<sub>2</sub> production rate during the negative polarization, proving that the catalytic  
2 deactivation is negligible and that there is no loss of potassium under the explored EPOC  
3 conditions. As it has been already reported [26,66], the continuous formation and adsorption of  
4 intermediate carbonaceous species could block catalyst active sites under steam reforming  
5 conditions leading to significant activity losses (resulting in a 50% drop of ethanol conversion in  
6 some cases [62,67]). Nonetheless and, in all cases, the addition of oxygen (autothermal reforming  
7 atmosphere) produced an appreciable improvement in the catalyst stability, as it has been proved  
8 comparing our previous study with those results shown in **Figure 6**, which in addition is  
9 compatible with the EPOC enhancement effect.

#### 10 **4. Conclusions**

11 To recapitulate, this study demonstrated the contribution of EPOC effect on remarkable  
12 enhancement of hydrogen production rate under ethanol partial oxidation conditions. Hence, the  
13 electrochemical supply of potassium ions into Pt catalyst film increases the hydrogen production  
14 rate due to a decrease in catalyst potential and catalyst work function. The migration of potassium  
15 ions weakened the Pt chemical bond with electron-donor adsorbates (ethanol) and strengthened  
16 chemical bond with electron-acceptor ones (oxygen).

17 As observed from temperature programmed reaction experiments, the negative polarization  
18 activated ethanol oxidation dehydrogenation into acetaldehyde and its further acetaldehyde  
19 reforming and decomposition reactions, and hence the rest of the mechanism for hydrogen  
20 production, allowing the further oxidation of acetaldehyde that could not be completed without the  
21 presence of potassium promoter ions. The promotional effect favored this route instead of ethanol  
22 dehydration reaction, which led to ethylene formation. It demonstrates the interest of EPOC for  
23 in-situ tuning catalyst selectivity toward a certain desired product along with having a better  
24 mechanistic view on involved catalytic reactions.

25 The expanding of this study to steam reforming and autothermal reforming conditions  
26 demonstrates that this latter reaction atmosphere shows the best behavior in terms of catalytic  
27 activity, stability and EPOC enhanced effect achieving an increase in the H<sub>2</sub> production rate of 1.6  
28 times vs. the un-promoted catalyst state. The reproducibility of the EPOC phenomenon was fully  
29 demonstrated as well as the stability of the catalyst film and promotional phases under electro-

1 promotion conditions. These results show potential for the practical use of the electrocatalytic  
2 configuration in the H<sub>2</sub> technology as well as the operando controlling of the H<sub>2</sub> production rate  
3 for mobile processes.

#### 4 **Credit authorship contribution statement**

5 **Arash Fella Jahromi:** Conceptualization, Methodology, Investigation, Writing original draft,  
6 Writing-review & editing, Visualization, Data curation. **Estela Ruiz-López:** Conceptualization,  
7 Methodology, Investigation, Writing original draft, Writing-review & editing, Visualization, Data  
8 curation. **Fernando Dorado:** Supervision, Writing-review & editing, Funding acquisition, Data  
9 curation. **Elena A. Baranova:** Supervision, Writing-review & editing, Funding acquisition, Data  
10 curation. **Antonio de Lucas-Consuegra:** Supervision, Writing-review & editing, Funding  
11 acquisition, Data curation.

#### 12 **Declaration of Competing Interest**

13 There are no known competing financial interests to declare.

#### 14 **Acknowledgments**

15 Authors would like to appreciate Mitacs for financial support of this research via Globalink  
16 Research Award (IT13784). In addition, the authors gratefully acknowledge Spanish Ministry of  
17 Science and Innovation for the financial support of this work [PID2019-107499RB-I00].

18

#### 19 **References**

- 20 [1] A. Sartbaeva, V.L. Kuznetsov, S.A. Wells, P.P. Edwards, Hydrogen nexus in a sustainable energy  
21 future, *Energy Environ. Sci.* 1 (2008) 79–85. <https://doi.org/10.1039/B810104N>.
- 22 [2] A. Campen, K. Mondal, T. Wiltowski, Separation of hydrogen from syngas using a regenerative  
23 system, *Int. J. Hydrogen Energy.* 33 (2008) 332–339.  
24 <https://doi.org/10.1016/j.ijhydene.2007.07.016>.
- 25 [3] A. Vita, L. Pino, C. Italiano, A. Palella, Steam reforming, partial oxidation, and autothermal  
26 reforming of ethanol for hydrogen production in conventional reactors, in: *Ethanol Sci. Eng.*,  
27 Elsevier, 2018: pp. 159–191. <https://doi.org/10.1016/B978-0-12-811458-2.00006-7>.
- 28 [4] J.L. Contreras, J. Salmones, J.A. Colín-Luna, L. Nuño, B. Quintana, I. Córdova, B. Zeifert, C.  
29 Tapia, G.A. Fuentes, Catalysts for H<sub>2</sub> production using the ethanol steam reforming (a review),  
30 *Int. J. Hydrogen Energy.* 39 (2014) 18835–18853. <https://doi.org/10.1016/j.ijhydene.2014.08.072>.
- 31 [5] F. Liu, L. Zhao, H. Wang, X. Bai, Y. Liu, Study on the preparation of Ni-La-Ce oxide catalyst for  
32 steam reforming of ethanol, *Int. J. Hydrogen Energy.* 39 (2014) 10454–10466.  
33 <https://doi.org/10.1016/j.ijhydene.2014.05.036>.

- 1 [6] J. Yu, J.A. Odriozola, T.R. Reina, Dry Reforming of Ethanol and Glycerol: Mini-Review,  
2 Catalysts. 9 (2019) 1015. <https://doi.org/10.3390/catal9121015>.
- 3 [7] G. yi Chen, W. qing Li, H. Chen, B. bei Yan, Progress in the aqueous-phase reforming of different  
4 biomass-derived alcohols for hydrogen production, J. Zhejiang Univ. Sci. A. 16 (2015) 491–506.  
5 <https://doi.org/10.1631/jzus.A1500023>.
- 6 [8] A. V. Tokarev, A. V. Kirilin, E. V. Murzina, K. Eränen, L.M. Kustov, D.Y. Murzin, J.P. Mikkola,  
7 The role of bio-ethanol in aqueous phase reforming to sustainable hydrogen, Int. J. Hydrogen  
8 Energy. 35 (2010) 12642–12649. <https://doi.org/10.1016/j.ijhydene.2010.07.118>.
- 9 [9] T. da Silva Veras, T.S. Mozer, D. da Costa Rubim Messeder dos Santos, A. da Silva César,  
10 Hydrogen: Trends, production and characterization of the main process worldwide, Int. J.  
11 Hydrogen Energy. 42 (2017) 2018–2033. <https://doi.org/10.1016/j.ijhydene.2016.08.219>.
- 12 [10] L. V. Mattos, F.B. Noronha, Partial oxidation of ethanol on supported Pt catalysts, J. Power  
13 Sources. 145 (2005) 10–15. <https://doi.org/10.1016/j.jpowsour.2004.12.034>.
- 14 [11] W. Cai, F. Wang, E. Zhan, A.C. Van Veen, C. Mirodatos, W. Shen, Hydrogen production from  
15 ethanol over Ir/CeO<sub>2</sub> catalysts: A comparative study of steam reforming, partial oxidation and  
16 oxidative steam reforming, J. Catal. 257 (2008) 96–107. <https://doi.org/10.1016/j.jcat.2008.04.009>.
- 17 [12] F. Auprêtre, C. Descorme, D. Duprez, Bio-ethanol catalytic steam reforming over supported metal  
18 catalysts, Catal. Commun. 3 (2002) 263–267. [https://doi.org/10.1016/S1566-7367\(02\)00118-8](https://doi.org/10.1016/S1566-7367(02)00118-8).
- 19 [13] R. Padilla, M. Benito, L. Rodríguez, A. Serrano, G. Muñoz, L. Daza, Nickel and cobalt as active  
20 phase on supported zirconia catalysts for bio-ethanol reforming: Influence of the reaction  
21 mechanism on catalysts performance, Int. J. Hydrogen Energy. 35 (2010) 8921–8928.  
22 <https://doi.org/10.1016/j.ijhydene.2010.06.021>.
- 23 [14] M. Greluk, M. Rotko, S. Turczyniak-Surdacka, Enhanced catalytic performance of La<sub>2</sub>O<sub>3</sub>  
24 promoted Co/CeO<sub>2</sub> and Ni/CeO<sub>2</sub> catalysts for effective hydrogen production by ethanol steam  
25 reforming: La<sub>2</sub>O<sub>3</sub> promoted Co(Ni)/CeO<sub>2</sub> catalysts in SRE, Renew. Energy. 155 (2020) 378–395.  
26 <https://doi.org/10.1016/j.renene.2020.03.117>.
- 27 [15] M. Bilal, S.D. Jackson, Ethanol steam reforming over Rh and Pt catalysts: Effect of temperature  
28 and catalyst deactivation, Catal. Sci. Technol. 3 (2013) 754–766.  
29 <https://doi.org/10.1039/c2cy20703f>.
- 30 [16] A. Le Valant, N. Bion, F. Can, D. Duprez, F. Epron, Preparation and characterization of bimetallic  
31 Rh-Ni/Y<sub>2</sub>O<sub>3</sub>-Al<sub>2</sub>O<sub>3</sub> for hydrogen production by raw bioethanol steam reforming: influence of the  
32 addition of nickel on the catalyst performances and stability, Appl. Catal. B Environ. 97 (2010)  
33 72–81. <https://doi.org/10.1016/j.apcatb.2010.03.025>.
- 34 [17] A.E.P. de Lima, D.C. de Oliveira, In situ XANES study of Cobalt in Co-Ce-Al catalyst applied to  
35 Steam Reforming of Ethanol reaction, Catal. Today. 283 (2017) 104–109.  
36 <https://doi.org/10.1016/j.cattod.2016.02.029>.
- 37 [18] V. Spallina, G. Maturro, C. Ruocco, E. Meloni, V. Palma, E. Fernandez, J. Melendez, A.D.  
38 Pacheco Tanaka, J.L. Viviente Sole, M. van Sint Annaland, F. Gallucci, Direct route from ethanol  
39 to pure hydrogen through autothermal reforming in a membrane reactor: Experimental  
40 demonstration, reactor modelling and design, Energy. 143 (2018) 666–681.  
41 <https://doi.org/10.1016/J.ENERGY.2017.11.031>.
- 42 [19] V. Palma, C. Ruocco, E. Meloni, A. Ricca, Oxidative reforming of ethanol over CeO<sub>2</sub>-SiO<sub>2</sub> based  
43 catalysts in a fluidized bed reactor, Chem. Eng. Process. - Process Intensif. 124 (2018) 319–327.

- 1 <https://doi.org/10.1016/J.CEP.2017.08.010>.
- 2 [20] C. Ruocco, V. Palma, A. Ricca, Hydrogen production by oxidative reforming of ethanol in a  
3 fluidized bed reactor using a Pt[ $\gamma$ -Ni]/CeO<sub>2</sub>[ $\gamma$ -SiO<sub>2</sub>] catalyst, *Int. J. Hydrogen Energy*. 44  
4 (2019) 12661–12670. <https://doi.org/10.1016/j.ijhydene.2018.12.154>.
- 5 [21] A. Nieto-Márquez, D. Sánchez, A. Miranda-Dahdal, F. Dorado, A. de Lucas-Consuegra, J.L.  
6 Valverde, Autothermal reforming and water-gas shift double bed reactor for H<sub>2</sub> production from  
7 ethanol, *Chem. Eng. Process. - Process Intensif.* 74 (2013) 14–18.  
8 <https://doi.org/10.1016/j.cep.2013.10.006>.
- 9 [22] V. Palma, C. Ruocco, E. Meloni, F. Gallucci, A. Ricca, Enhancing Pt-Ni/CeO<sub>2</sub> performances for  
10 ethanol reforming by catalyst supporting on high surface silica, *Catal. Today*. 307 (2018) 175–188.  
11 <https://doi.org/10.1016/J.CATTOD.2017.05.034>.
- 12 [23] M. Taghizadeh, F. Aghili, Recent advances in membrane reactors for hydrogen production by  
13 steam reforming of ethanol as a renewable resource, *Rev. Chem. Eng.* 35 (2019) 377–392.  
14 <https://doi.org/10.1515/revce-2017-0083>.
- 15 [24] J.Y.Z. Chiou, J.Y. Siang, S.Y. Yang, K.F. Ho, C.L. Lee, C.T. Yeh, C. Bin Wang, Pathways of  
16 ethanol steam reforming over ceria-supported catalysts, in: *Int. J. Hydrogen Energy*, 2012: pp.  
17 13667–13673. <https://doi.org/10.1016/j.ijhydene.2012.02.081>.
- 18 [25] A.M. Silva, L.O.O. Costa, A.P.M.G. Barandas, L.E.P. Borges, L. V. Mattos, F.B. Noronha, Effect  
19 of the metal nature on the reaction mechanism of the partial oxidation of ethanol over CeO<sub>2</sub>-  
20 supported Pt and Rh catalysts, *Catal. Today*. 133–135 (2008) 755–761.  
21 <https://doi.org/10.1016/j.cattod.2007.12.103>.
- 22 [26] S.M. De Lima, A.M. Da Silva, L.O.O. Da Costa, U.M. Graham, G. Jacobs, B.H. Davis, L. V.  
23 Mattos, F.B. Noronha, Study of catalyst deactivation and reaction mechanism of steam reforming,  
24 partial oxidation, and oxidative steam reforming of ethanol over Co/CeO<sub>2</sub> catalyst, *J. Catal.* 268  
25 (2009) 268–281. <https://doi.org/10.1016/j.jcat.2009.09.025>.
- 26 [27] E. Kraleva, C.P. Rodrigues, M.M. Pohl, H. Ehrich, F.B. Noronha, Syngas production by partial  
27 oxidation of ethanol on PtNi/SiO<sub>2</sub>-CeO<sub>2</sub> catalysts, *Catal. Sci. Technol.* 9 (2019) 634–645.  
28 <https://doi.org/10.1039/c8cy02418a>.
- 29 [28] V.A. Sadykov, N.F. Ereemeev, E.M. Sadovskaya, Y.A. Chesalov, S.N. Pavlova, V.A. Rogov, M.N.  
30 Simonov, A.S. Bobin, T.S. Glazneva, E.A. Smal, A.I. Lukashevich, A. V. Krasnov, V.I. Avdeev,  
31 A.C. Roger, Detailed Mechanism of Ethanol Transformation into Syngas on Catalysts Based on  
32 Mesoporous MgAl<sub>2</sub>O<sub>4</sub> Support Loaded with Ru + Ni/(PrCeZrO or MnCr<sub>2</sub>O<sub>4</sub>) Active  
33 Components, *Top. Catal.* 63 (2020) 166–177. <https://doi.org/10.1007/s11244-020-01222-1>.
- 34 [29] A.M. Silva, A.M.D. de Farias, L.O.O. Costa, A.P.M.G. Barandas, L. V. Mattos, M.A. Fraga, F.B.  
35 Noronha, Partial oxidation and water-gas shift reaction in an integrated system for hydrogen  
36 production from ethanol, *Appl. Catal. A Gen.* 334 (2008) 179–186.  
37 <https://doi.org/10.1016/j.apcata.2007.10.004>.
- 38 [30] D. Yun, Y. Zhao, I. Abdullahi, J.E. Herrera, The effect of interstitial nitrogen in the activity of the  
39 VO<sub>x</sub>/N-TiO<sub>2</sub> catalytic system for ethanol partial oxidation, *J. Mol. Catal. A Chem.* 390 (2014)  
40 169–177. <https://doi.org/10.1016/j.molcata.2014.03.022>.
- 41 [31] R.J. Chimentão, J.E. Herrera, J.H. Kwak, F. Medina, Y. Wang, C.H.F. Peden, Oxidation of ethanol  
42 to acetaldehyde over Na-promoted vanadium oxide catalysts, *Appl. Catal. A Gen.* 332 (2007) 263–  
43 272. <https://doi.org/10.1016/j.apcata.2007.08.024>.

- 1 [32] M. Stoukides, C.G. Vayenas, The effect of electrochemical oxygen pumping on the rate and  
2 selectivity of ethylene oxidation on polycrystalline silver, *J. Catal.* 70 (1981) 137–146.  
3 [https://doi.org/10.1016/0021-9517\(81\)90323-7](https://doi.org/10.1016/0021-9517(81)90323-7).
- 4 [33] C. Vayenas, S. Bebeli, C. Pliangos, S. Brosda, D. Tsiplakides, *Electrochemical activation of*  
5 *catalysis: promotion, electrochemical promotion, and metal-support interactions*, Springer Science  
6 & Business Media, 2001.
- 7 [34] P. Vernoux, L. Lizarraga, M.N. Tsampas, F.M. Sapountzi, A. De Lucas-Consuegra, J.L. Valverde,  
8 S. Souentie, C.G. Vayenas, D. Tsiplakides, S. Balomenou, E.A. Baranova, Ionically conducting  
9 ceramics as active catalyst supports, *Chem. Rev.* 113 (2013) 8192–8260.  
10 <https://doi.org/10.1021/cr4000336>.
- 11 [35] C. Panaritis, J. Zgheib, S.A.H. Ebrahim, M. Couillard, E.A. Baranova, Electrochemical in-situ  
12 activation of Fe-oxide nanowires for the reverse water gas shift reaction, *Appl. Catal. B Environ.*  
13 269 (2020) 118826. <https://doi.org/10.1016/j.apcatb.2020.118826>.
- 14 [36] D. Zagoraios, C. Panaritis, A. Krassakopoulou, E.A. Baranova, A. Katsaounis, C.G. Vayenas,  
15 Electrochemical promotion of Ru nanoparticles deposited on a proton conductor electrolyte during  
16 CO<sub>2</sub> hydrogenation, *Appl. Catal. B Environ.* 276 (2020) 119148.  
17 <https://doi.org/10.1016/j.apcatb.2020.119148>.
- 18 [37] A. De Lucas-Consuegra, A. Caravaca, P.J. Martínez, J.L. Endrino, F. Dorado, J.L. Valverde,  
19 Development of a new electrochemical catalyst with an electrochemically assisted regeneration  
20 ability for H<sub>2</sub> production at low temperatures, *J. Catal.* 274 (2010) 251–258.  
21 <https://doi.org/10.1016/j.jcat.2010.07.007>.
- 22 [38] J. González-Cobos, D. López-Pedrajas, E. Ruiz-López, J.L. Valverde, A. de Lucas-Consuegra,  
23 Applications of the electrochemical promotion of catalysis in methanol conversion processes, *Top.*  
24 *Catal.* 58 (2015) 1290–1302. <https://doi.org/10.1007/s11244-015-0493-7>.
- 25 [39] J. González-Cobos, V.J. Rico, A.R. González-Elipse, J.L. Valverde, A. De Lucas-Consuegra,  
26 Electrochemical activation of an oblique angle deposited Cu catalyst film for H<sub>2</sub> production,  
27 *Catal. Sci. Technol.* 5 (2015) 2203–2214. <https://doi.org/10.1039/c4cy01524j>.
- 28 [40] S. Souentie, L. Lizarraga, A. Kambolis, M. Alves-Fortunato, J.L. Valverde, P. Vernoux,  
29 Electrochemical promotion of the water-gas shift reaction on Pt/YSZ, *J. Catal.* 283 (2011) 124–  
30 132. <https://doi.org/10.1016/j.jcat.2011.07.009>.
- 31 [41] A. De Lucas-Consuegra, A. Caravaca, J. González-Cobos, J.L. Valverde, F. Dorado,  
32 Electrochemical activation of a non noble metal catalyst for the water-gas shift reaction, *Catal.*  
33 *Commun.* 15 (2011) 6–9. <https://doi.org/10.1016/j.catcom.2011.08.007>.
- 34 [42] I. V. Yentekakis, Y. Jiang, S. Neophytides, S. Bebelis, C.G. Vayenas, Catalysis, electrocatalysis  
35 and electrochemical promotion of the steam reforming of methane over Ni film and Ni-YSZ  
36 cermet anodes, *Ionics (Kiel)*. 1 (1995) 491–498. <https://doi.org/10.1007/BF02375296>.
- 37 [43] A. Caravaca, A. De Lucas-Consuegra, C. Molina-Mora, J.L. Valverde, F. Dorado, Enhanced H<sub>2</sub>  
38 formation by electrochemical promotion in a single chamber steam electrolysis cell, *Appl. Catal. B*  
39 *Environ.* 106 (2011) 54–62. <https://doi.org/10.1016/j.apcatb.2011.05.004>.
- 40 [44] J. González-Cobos, J.L. Valverde, A. de Lucas-Consuegra, Electrochemical vs. chemical  
41 promotion in the H<sub>2</sub> production catalytic reactions, *Int. J. Hydrogen Energy*. 42 (2017) 13712–  
42 13723. <https://doi.org/10.1016/j.ijhydene.2017.03.085>.
- 43 [45] A. Caravaca, J. González-Cobos, P. Vernoux, A Discussion on the Unique Features of

- 1 Electrochemical Promotion of Catalysis (EPOC): Are We in the Right Path Towards Commercial  
2 Implementation?, *Catal.* 2020, Vol. 10, Page 1276. 10 (2020) 1276.  
3 <https://doi.org/10.3390/CATAL10111276>.
- 4 [46] E.R. López, F. Dorado, A. de Lucas-Consuegra, Electrochemical promotion for hydrogen  
5 production via ethanol steam reforming reaction, *Appl. Catal. B Environ.* 243 (2019) 355–364.  
6 <https://doi.org/10.1016/j.apcatb.2018.10.062>.
- 7 [47] S. Douvartzides, K. Kyriakopoulos, P. Tsiakaras, Electrochemical promotion of Pt during the  
8 oxidation of ethanol, *Ionics (Kiel)*. 7 (2001) 237–240. <https://doi.org/10.1007/BF02419236>.
- 9 [48] P.E. Tsiakaras, S.L. Douvartzides, A.K. Demin, V.A. Sobyenin, The oxidation of ethanol over Pt  
10 catalyst-electrodes deposited on ZrO<sub>2</sub> (8 mol% Y<sub>2</sub>O<sub>3</sub>), in: *Solid State Ionics*, Elsevier, 2002: pp.  
11 721–726. [https://doi.org/10.1016/S0167-2738\(02\)00415-0](https://doi.org/10.1016/S0167-2738(02)00415-0).
- 12 [49] F. Dorado, A. de Lucas-Consuegra, P. Vernoux, J.L. Valverde, Electrochemical promotion of  
13 platinum impregnated catalyst for the selective catalytic reduction of NO by propene in presence  
14 of oxygen, *Appl. Catal. B Environ.* 73 (2007) 42–50. <https://doi.org/10.1016/j.apcatb.2006.12.001>.
- 15 [50] I. V. Yentekakis, S. Bebelis, Study of the NEMCA effect in a single-pellet catalytic reactor, *J.*  
16 *Catal.* 137 (1992) 278–283. [https://doi.org/10.1016/0021-9517\(92\)90157-D](https://doi.org/10.1016/0021-9517(92)90157-D).
- 17 [51] F.J. Williams, N. Macleod, M.S. Tikhov, R.M. Lambert, Electrochemical promotion of bimetallic  
18 Rh-Ag/YSZ catalysts for the reduction of NO under lean burn conditions, *Electrochim. Acta.* 47  
19 (2002) 1259–1265. [https://doi.org/10.1016/S0013-4686\(01\)00856-8](https://doi.org/10.1016/S0013-4686(01)00856-8).
- 20 [52] P. Vernoux, F. Gaillard, C. Lopez, E. Siebert, Coupling catalysis to electrochemistry: A solution to  
21 selective reduction of nitrogen oxides in lean-burn engine exhausts?, *J. Catal.* 217 (2003) 203–208.  
22 [https://doi.org/10.1016/S0021-9517\(03\)00052-6](https://doi.org/10.1016/S0021-9517(03)00052-6).
- 23 [53] I. V. Yentekakis, M. Konsolakis, R.M. Lambert, N. MacLeod, L. Nalbantian, Extraordinarily  
24 effective promotion by sodium in emission control catalysis: NO reduction by propene over Na-  
25 promoted Pt/ $\gamma$ -Al<sub>2</sub>O<sub>3</sub>, *Appl. Catal. B Environ.* 22 (1999) 123–133. [https://doi.org/10.1016/S0926-3373\(99\)00042-9](https://doi.org/10.1016/S0926-3373(99)00042-9).
- 27 [54] A. De Lucas-Consuegra, J. González-Cobos, Y. García-Rodríguez, A. Mosquera, J.L. Endrino,  
28 J.L. Valverde, Enhancing the catalytic activity and selectivity of the partial oxidation of methanol  
29 by electrochemical promotion, *J. Catal.* 293 (2012) 149–157.  
30 <https://doi.org/10.1016/j.jcat.2012.06.016>.
- 31 [55] D.K. Liguras, K. Goundani, X.E. Verykios, Production of hydrogen for fuel cells by catalytic  
32 partial oxidation of ethanol over structured Ni catalysts, *J. Power Sources.* 130 (2004) 30–37.  
33 <https://doi.org/10.1016/j.jpowsour.2003.12.008>.
- 34 [56] L. V. Mattos, F.B. Noronha, Hydrogen production for fuel cell applications by ethanol partial  
35 oxidation on Pt/CeO<sub>2</sub> catalysts: The effect of the reaction conditions and reaction mechanism, *J.*  
36 *Catal.* 233 (2005) 453–463. <https://doi.org/10.1016/j.jcat.2005.04.022>.
- 37 [57] L. V. Mattos, F.B. Noronha, The influence of the nature of the metal on the performance of cerium  
38 oxide supported catalysts in the partial oxidation of ethanol, *J. Power Sources.* 152 (2005) 50–59.  
39 <https://doi.org/10.1016/j.jpowsour.2004.12.052>.
- 40 [58] J.P. Espinós, V.J. Rico, J. González-Cobos, J.R. Sánchez-Valencia, V. Pérez-Dieste, C. Escudero,  
41 A. de Lucas-Consuegra, A.R. González-Elipé, In situ monitoring of the phenomenon of  
42 electrochemical promotion of catalysis, *J. Catal.* 358 (2018) 27–34.  
43 <https://doi.org/10.1016/j.jcat.2017.11.027>.

- 1 [59] B. Sawatmongkhon, K. Theinnoi, T. Wongchang, C. Haoharn, C. Wongkhorsub, A. Tsolakis,  
2 Hydrogen production via the catalytic partial oxidation of ethanol on a platinum-rhodium catalyst:  
3 Effect of the oxygen-to-ethanol molar ratio and the addition of steam, *Energy and Fuels*. 33 (2019)  
4 6742–6753. <https://doi.org/10.1021/acs.energyfuels.9b01398>.
- 5 [60] M. Schmal, D. V. Cesar, M.M.V.M. Souza, C.E. Guarido, Drifts and TPD analyses of ethanol on  
6 Pt catalysts over  $\text{Al}_2\text{O}_3$  and  $\text{ZrO}_2$  —partial oxidation of ethanol, *Can. J. Chem. Eng.* 89 (2011)  
7 1166–1175. <https://doi.org/10.1002/cjce.20597>.
- 8 [61] K.L. Hohn, Y.C. Lin, Catalytic partial oxidation of methanol and ethanol for hydrogen generation,  
9 *ChemSusChem*. 2 (2009) 927–940. <https://doi.org/10.1002/cssc.200900104>.
- 10 [62] S. Cavallaro, V. Chiodo, S. Freni, N. Mondello, F. Frusteri, Performance of Rh/Al<sub>2</sub>O<sub>3</sub> catalyst in  
11 the steam reforming of ethanol: H<sub>2</sub> production for MCFC, *Appl. Catal. A Gen.* 249 (2003) 119–  
12 128. [https://doi.org/10.1016/S0926-860X\(03\)00189-3](https://doi.org/10.1016/S0926-860X(03)00189-3).
- 13 [63] Y.F.Y. Yao, Catalytic Oxidation of Ethanol at Low Concentrations, *Ind. Eng. Chem. Process Des.*  
14 *Dev.* 23 (1984) 60–67. <https://doi.org/10.1021/i200024a011>.
- 15 [64] L.O.O. Costa, A.M. Silva, L.E.P. Borges, L. V. Mattos, F.B. Noronha, Partial oxidation of ethanol  
16 over Pd/CeO<sub>2</sub> and Pd/Y<sub>2</sub>O<sub>3</sub> catalysts, *Catal. Today*. 138 (2008) 147–151.  
17 <https://doi.org/10.1016/j.cattod.2008.05.003>.
- 18 [65] D. Livio, C. Diehm, A. Donazzi, A. Beretta, O. Deutschmann, Catalytic partial oxidation of  
19 ethanol over Rh/Al<sub>2</sub>O<sub>3</sub>: Spatially resolved temperature and concentration profiles, *Appl. Catal. A*  
20 *Gen.* 467 (2013) 530–541. <https://doi.org/10.1016/j.apcata.2013.07.054>.
- 21 [66] S.M. de Lima, I.O. da Cruz, G. Jacobs, B.H. Davis, L. V Mattos, F.B. Noronha, Steam reforming,  
22 partial oxidation, and oxidative steam reforming of ethanol over Pt/CeZrO<sub>2</sub> catalyst, *J. Catal.* 257  
23 (2008) 356–368. <https://doi.org/10.1016/j.jcat.2008.05.017>.
- 24 [67] S. Cavallaro, V. Chiodo, A. Vita, S. Freni, Hydrogen production by auto-thermal reforming of  
25 ethanol on Rh/Al<sub>2</sub>O<sub>3</sub> catalyst, *J. Power Sources*. 123 (2003) 10–16.  
26 [https://doi.org/10.1016/S0378-7753\(03\)00437-3](https://doi.org/10.1016/S0378-7753(03)00437-3).

27

28

29

30